ISSN (Print) : 0974-6846
Indian Journal of Science and Technology, Vol 8(28), DOI: 10.17485/ijst/2015/v8i28/81818, October 2015 ISSN (Online) : 0974-5645

The Sedimentation of Slim Flexible Particles in Stokes Flow

Behzad Shojaei* **and Hamid Dehghani**

Department of Engineering, Malek-Ashtar University of Technology, Lavizan, Tehran - 15875 1774, Iran;
bshojaei@mail.kntu.ac.ir, hamid_deh@yahoo.com

Abstract

Background/Objectives: The dynamics of elastic slim particles (filaments) surrounded by fluid flow is a noteworthy topic of study because of its application in natural sciences and industrial processes. When deformation of elastic particle is large many complications arise which needs specific consideration in order to develop an efficient method for modeling the solid-fluid interaction accurately and with acceptable computational cost. **Method:** In order to study the sedimentation process of filament which is immersed in a quiescent fluid flow, we constitute related governing equations based on non-local solid-fluid interaction coupling with slender body theory. The fluid flow governed by Stokes assumptions which allow us to use superposition principle. Also, the extracted equations rearrange by two controller parameters Elasto-gravitation, β, and Slenderness-parameter, ϵ. **Findings:** A Highly Flexible filament (HF-filament) and a Moderately Flexible filament (MF-filament) have examined by mentioned method. The results show that the HF-filament fall on a periodic motion during the sedimentation process. This periodic motion leads to a set of unbalance forces along the filament which causes a permanent lateral drift. In the other side the MF-filament meets an equilibrium point with a final constant U-shape. Also, in order to validation we compare the outcome data with the results obtained by local and multiple scale analysis methods. **Application/Improvements:** The approach have been presented by this paper can be used in different fields which there are any necessity to simulating slim particles motion more simple and with less computational cost in compare with conventional methods.

Keywords: Elastic Buckling Instability, Flexible Filament, Non-Local Method, Slender Body Theory, Stokes Flow

1. Introduction

The dynamics of solid-fluid compound system is an important topic of study because of its role in many natural and industrial areas such as biological issues[1,2] pulp and papermaking industry[3] and etc. A vast literature can be found which carried out to understand the dynamics of rigid or flexible bodies in simple or complex shapes surrounded by a quiescent or moving fluid. In many cases the papers focused on systems included small particles immersed in an incompressible fluid governed by Stokes assumptions. In 1851, Stokes presented a formula for the settling speed of a solid sphere[4]. Stimson and Jeffery[5] studied the motion of two similar spheres sediment in a quiescent fluid. They concluded that the nonlocal interaction between spheres, which is mediated by fluid, leads to increasing the settling speed. With development of numerical and experimental methods the investigations had led to simulating the ellipsoidal and slim particles[6,7]. Then the studies had gone to model deformable objects with different aspect ratios[8–12].

A body conforming grid is being used for computing the flow around an immersed object in conventional methods. These approaches are not efficient and require complex grid generation in cases with large body deformation[13]. To treat this difficulty, many numerical

* Author for correspondence

methods have been proposed for modeling the interaction between viscous forces in a fluid flow and elastic stresses in deformable objects immersed in the fluid flow. Among all of them, the methods are based on non-body conforming Cartesian grid gain most attention due to their application in majority of fluid-structure problems. The most popular of these methods is Immersed Boundary Method (IBM) developed by Peskin[14] which can be categorized as a grid-based method. In IBM fluid motion is simulated by Eulerian approach while Lagrangian method use for tracking the solid. Slim particle behaviours are studied in several papers by IBM, e.g.[3,15]. The IBM has bad reputation in numerical convergence due to the stiffness of its extracted equations. Hence, the numerical process requires small time-steps to maintain stability, which leads to high computational cost[16]. One possible way to treat such difficulties is to employ Stokes flow assumptions incase with low Reynolds number.

Generally, Stokes flow is utilized to simulating the fluid-solid interaction without any necessity for meshing the fluid domain. In order to deal with slim particles (filaments), small Slenderness-Parameter (SP), several methods are developed based on Slender Body Theory (SBT) and superposition rule which is allowed due to linearity property of governing equation extracted by employing Stokes flow assumptions, i.e. neglecting inertia terms. In this method the forces are asymptotically expanded in powers of SP, then after some complex mathematical procedure some series came out for the forces which the first term is associated with local interaction and the others are related to non-local interactions mediated by the incompressible fluid intervening and can be neglected in cases with special situation.

The model which includes only the first term of the expansion is refereed as Local Model (LM). This model employed by Becker and Shelley[17] to simulate the dynamic of a high SP flexible filament rotates in viscous linear shear flow. Also Dehghani and Shojaei[18] have utilized a version of LM to study the sedimentation process of single flexible filament for different SPs. Further information about the difference between LM and n-LM, also the definition of three types of filament, Weakly Flexible filament (WF-filament), Moderately Flexible filament (MF-filament) and Highly Flexible filament (HF-filament), can be find in[11,18].

In some cases the non-local interactions have significant effect on the dynamic of particles whose dynamics are under investigation. Keller and Rubinow[19] elicited an integral equation for the viscous force per unit length exerted on centerline of the body by utilizing asymptotically matching expansion based on n-LM. They used the n-LM to study a viscous and incompressible flow past a slim body in low Reynolds number. Shelley and Ueda[20] used a modified version of n-LM to simulate a growing liquid crystal.

In 2004, a perfect paper about the dynamics of flexible filaments using n-LM is published by Tornberg and Shelley[11]. They examined a set of filaments with free end suspended in a simple shear flow using an integral equation extracted by taking into account all kinds of interactions, i.e. fluid-solid and solid-solid. They presented novel approaches to overcome the singularities exist in non-local integral equations.

Recently some analytical methods get attention by researchers in order to find an analytical expression for slim particle movements. Li et al.[21] evolved exact equations for dynamics of WF-filaments sediment in a quiescent fluid flow using multiple-scaled analysis. Also they took advantage of Tornberg and Shelley approaches to validate their results. They introduced elasto-gravitation number, β, to describe the ratio between elastic and viscous forces brought on by gravity.

In present study two types of filaments, Moderately Flexible filament (MF-filament) and Highly Flexible filament (HF-filament) have been examined using non-local model and the Euler-Bernoulli theory to simulate the interactions and the filament internal forces, respectively. We have used Tornberg and Shelley approaches to tackle the singularities caused by non-local operator. Also as results of this study, the trajectory, deformation and transport diagram are plotted for filaments with straight initial form in different initial angles.

2. Methodology

Consider a flexible filament having total length L with centerline referred by *s*. In order to extract the governing equations, the Euler-Bernoulli beam model is used to describe the internal forces; also we neglect the twist elasticity. The final equation for internal forces obtains from encompassing following assumption in addition with having a uniform material distribution across the filaments with a two-dimensional position vector, $x(s, t) = [x(s, t), y(s, t)]^T$, which represents the filament centerline coordinate at a certain time.

$$f(s) = (EIx_{ss})_{ss} - (T(s)x_s)_s - F_g(s) \quad (1)$$

Here, $I(s) = \pi D^4/64$ is area moment of inertia, E represents elastic modulus, and the subscript s denotes differentiation with respect to arc length. Also the filaments examined in present study have uniform cross section area. In above equation first term shows bending stiffness of filament, second term acts as a Lagrange multiplier, see[11,17], and the last term stands for buoyancy forces which given by Archimedes' principle,

$$F_g(s) = \frac{\pi D^2}{4}(\rho\ filament - \rho\ fluid)g\begin{bmatrix}0\\-1\end{bmatrix} \quad (2)$$

Where g > 0 denotes the gravitational acceleration and ρ shows the densities. The total gravitational force along the filament, F_G, is given by summation of internal filament forces along the filament.

$$\int_0^L fds = -\int_0^L F_g(s)ds = -F_G \quad (3)$$

We non-dimensionalize the problem using filament length L and net gravitational force $|F_G|$. The non-dimensional equations are controlled by two parameters, Elasto-gravitation number (β) which represent a ratio between filament elastic force and gravitational force, and Slenderness parameter ($\epsilon = D/L$)

$$f^*(s^*) = \beta(EI^* x^*_{s^*s^*})_{s^*s^*} - (T^*(s^*)x^*_{s^*})_{s^*} - F_g^*(s^*)$$
$$I^* = 64I/\pi ED^4,\ T^* = T/|F_G|,\ s^* = s/L, x^* = x/L, \beta = \pi ED^4/64|F_G|_{L^2} \quad (4)$$

2.1 Non-Local Slender Body Equation

According to the slender body theory, a filament can be represented by a set of doublets and Stokeslets along the filament centerline, see[21]. Johnson[20] used this theory to evolve a system of equations which makes relation between filament velocity and the forces exerted on filament. For quiescent and incompressible fluid flow the relation is given by,

$$x^*_{t^*} = -\Lambda[f^*] - K[f^*] \quad (5)$$

Here, $t^* = t|F_G|/(8\pi\mu L^2)$ denotes dimensionless time and the local operator **Λ** and the non-local operator **K** have following arrangements.

$$\Lambda[f^*] = [-c(s^*)(I + x^*_{s^*} \otimes x^*_{s^*}) + 2(I - x^*_{s^*} \otimes x^*_{s^*})], f^*(s^*)$$

$$K[f^*] = \int_0^1 \left(\frac{I + \hat{R}(s^*, s^{*\prime}) \otimes \hat{R}(s^*, s^{*\prime})}{|R(s^*, s^{*\prime})|} f(s') - \frac{I + x_{s^*}(s^*) \otimes x_{s^*}(s^*)}{|s^* - s^{*\prime}|} f(s^*) \right) ds^{*\prime} \quad (6)$$

In above equations, ⊗ denotes dyadic product of two vectors, **I** is the identity tensor, $R(s,s') = x(s,t) - x(s',t), \hat{R}(s,s')$ the unit vector $\hat{R} = R/|R|$, and c is asymptotical parameter which is given by,

$$c(s^*) = 2\ln\left(\frac{D}{2L}\right) - \ln\left(\frac{2}{L}\sqrt{s(L-s)}\right) + 1 \quad (7)$$

Due to simplicity the superscripts, *, drop in the rest of paper.

In order to close the equations we need four boundary conditions for Equation (5) and an extra relation for filament internal tension, T(s). To this end, a second order linear equation can be obtained by filament inextensibility, x_s, $x_s = 1$. Also, the filament ends are free and no force or moments acting on them, these conditions lead to six BCs, Equation (9), i.e. two extra BCs need for tension equation, Eq. 8.

$$2cT_{ss} + (2-c)x_{ss}, x_{ss}T + 2c_sT_s = (2-7c)\beta EIx_{ss}, x_{ssss} - 6c\beta eIx_{sss}, x_{sss}$$
$$-\beta E6c_s, Ix_{ss}, x_{ssss} - (2+c)x_{ss}, F_g - 2c_sx_s, F_g \quad (8)$$

$$x_{ss}|_{s=0,1} = x_{sss}|_{s=0,1} = 0, \quad T|_{s=0,1} = 0 \quad (9)$$

The non-dimensional gravity force for uniform cross sectional area filament is given by $F_g = \begin{bmatrix}0\\-1\end{bmatrix}$.

2.2 Numerical Approach

Generally, the methods are evolved using stokes assumptions are simple to do because of superposition principle allowed due to the linear property of stokes flow. Nevertheless, in order to solve the extracted governing equations in previous section we need some special treatments to overcome the stiffness came out thru the fourth order derivative of filament position, $\mathbf{X}_{ssss}$. Furthermore, in integral equation of non-local operator, **K**[**f**], The denominator of first and second term go to zero when $s^s = s$. In order to get rid of the singularities and the stiffness we used a regularization process and a semi-implicit approach, respectively. Further details about regularization process and the semi-implicit approach, which have been employed, can be found in Zhu and Peskin[14], also the solution algorithm used to solve the governing equation in this paper is the same with the one we proposed in Dehghani and Shojaei[18].

3. Results and Discussion

Consider a flexible filament with orientation as shown

in Figure 1. The filament initially is straight with specific angle respect to horizon direction. Two types of filament have been investigated in this section. Due to have a comprehensive survey we have chosen the controller parameters in a way that a filament has stable behavior and other filament shows an unstable motion during the sedimentation process. Before start to present the results obtained from the solution of governing equations for two mentioned filaments, a comparison between local, non-local and multiple-scale analysis have been done, Figure 2. The data owing to Figure 2 are related to a Weakly Flexible filament (WF-filament) which its initial orientation is 63π/64. The controller parameters for a WF-filament can be set out as $\beta = 0.02$ and $\varepsilon = 0.01$. The procedures to obtain the data are discussed by us in Dehghani and Shojaei[18].

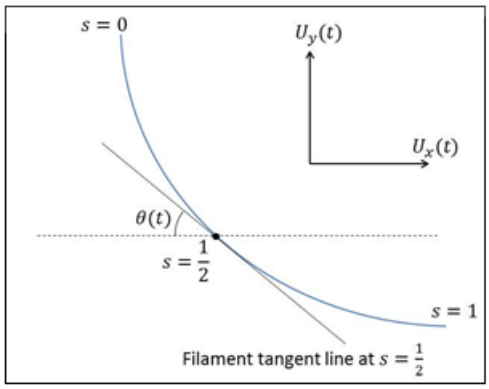

Figure 1. Illustration of a flexible filament (curved line).

Now, In order to have a MF-filament the controller parameters set out as $\beta = 0.0014$ and $\varepsilon = 10^{-4}$. Although a solid-fluid system with such properties would leads to large deformation in filament shape, it would not have instable behavior. The results are gain in different initial orientation and are shown in Figure 3-5. As can be seen in Figure 3 the filament has a lateral drift until it settles down to its stable situation and tends to a vertical line. Figure 4 shows the deformation and reorientation of MF-filament in a reference frame moving sets out to filament midpoint. As the filament deforms the internal forces change during the sedimentation until the filament meets its equilibrium point. In order to demonstrate the variation of internal forces, the tension diagram is plotted in Figure 5 during the sedimentation process.

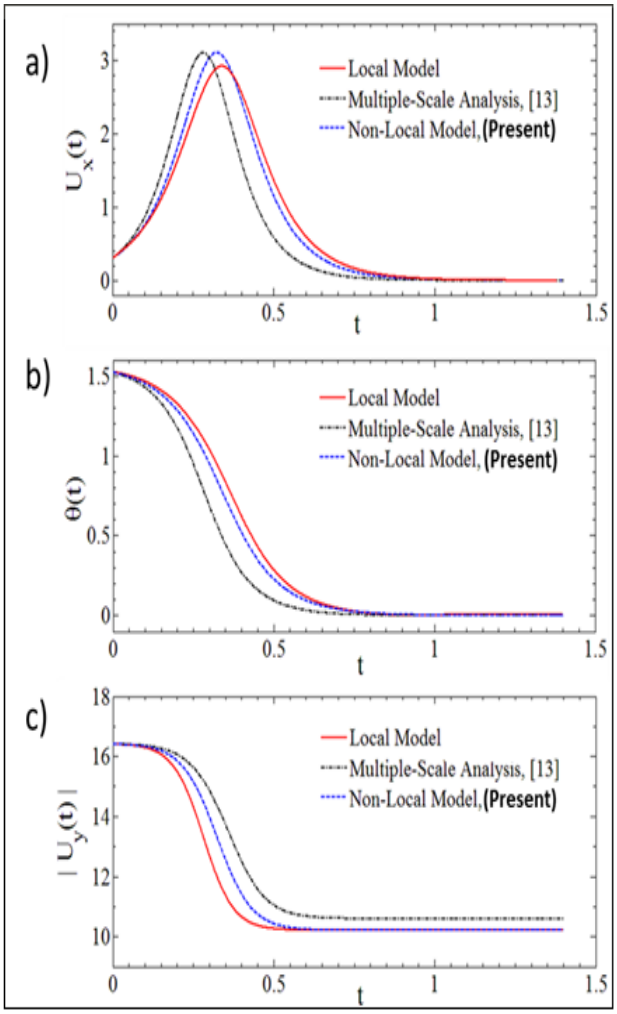

Figure 2. The results of three different methods obtained for a WF-filament with $\beta = 0.02$ and $\varepsilon = 0.01$.

- Horizontal filament velocity $U_x(t)$.
- Filament orientation $\theta(t)$.
- Downward filament velocity $|U_y(t)|$.

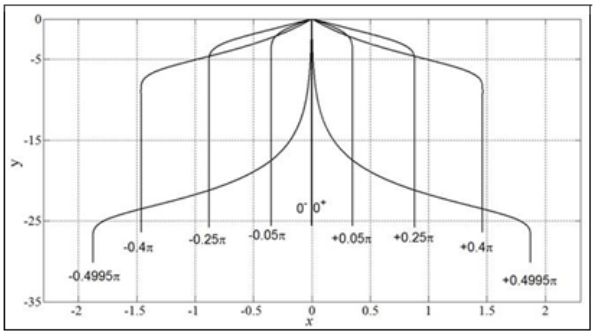

Figure 3. Trajectory diagrams of MF-filament in different initial orientation, $\beta = 0.0014$ and $\varepsilon = 10^{-4}$.

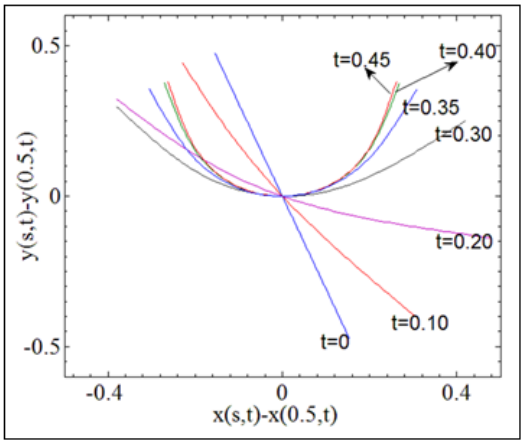

Figure 4. Deformation and transport of MF-filament during sedimentation in a reference frame moving with filament midpoint, $\theta_0 = \theta.4\pi$, $\beta = 0.0014$, $\varepsilon = 10^{-4}$, "t" show dimensionless time.

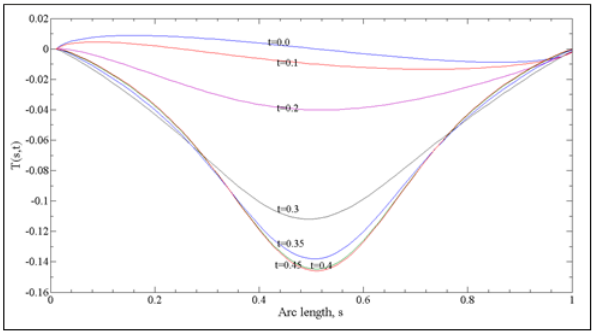

Figure 5. Variation of internal tension for MF-filament during the sedimentation process with $\theta_0 = \theta.4\pi$, "t" show dimensionless time

Here, we have been focused on a flexible filament which does not reach to equilibrium and shows instability during the sedimentation. Generally, the instability occurs when a perturbation imposed to an object (here the filament) cannot damp because the cause of damping (here bending rigidity of filament) is not large enough to overcome the cause of perturbation (here the forces induced by fluid and gravity). Thus, the body will not meet a stable situation.

In order to have a HF-filament the controller parameters set out as $\beta = 5.4 \times 10^{-5}$. As can be seen in Figure 6(a), the HF-filament initially acts almost like the MF-filament; however when it becomes more bend and more close to the horizontal situation the instability starts slowly. After a transient period which does not have any specific character the filament start a periodic motion with constant frequency which continue to end of sedimentation process. Also, the instability induces a forward lateral moving in filament which tends to an oblique asymptote. Figure 6(b) shows deformation and transportation of HF-filament over a period, the black points show the mid-point of filament. Note that the black points go forward and backward during the sedimentation, but at the end of period the last point goes further from the first one. This cradle motion explains all the matters about trajectory diagrams in Figure 6(a). Besides, the dimensionless time taken for each period is 0.056. We split up the dimensionless time period in ten segments, so that the dimensionless time over a period is given by,

$$t = t_n = 0.056\frac{n}{10}, \quad n = 0,1,2,.....,10 \tag{11}$$

The deformation of HF-filament over a period in a reference frame moving with midpoint of filament is shown in Figure 7. Also, it can be seen that the filament has two arms, a flapping arm and a stable arm. A set of unbalance force is emerged due to this asymmetrical behavior. These forces are like locomotion power which fish produce by flapping their tail. So, the flapping arm acts as fish tail and push forward the filament. Which one of two arms flaps is depends on the initial orientation of filament. Figure 8 shows the sedimentation of HF-filament in three different initial orientations over nineteen time-steps, as can be seen in this figure, contrary to cases with $\theta_0 = 0.25\pi, 0.1\pi$, which the right arm flaps, in case with $\theta_0 = 0.25\pi$ the flapping arm is the right one. In order to demonstrate the variation of internal forces, the tension diagram is plotted in Figure 9 over a period.

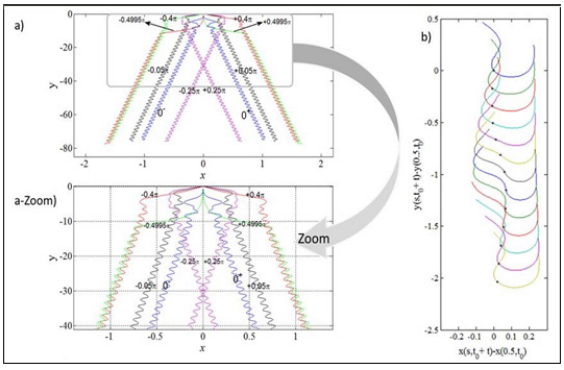

Figure 6. (a) Trajectory diagrams of MF-filament in different initial orientation. (b) Cradle motion of HF-filament over a period, the black points show mid-point of the filament, $\beta = 5.4 \times 10^{-5}$ and $\varepsilon = 2 \times 10^{-5}$.

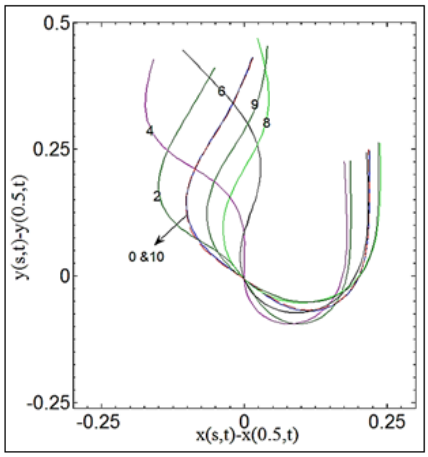

Figure 7. Deformation and transport of HF-filament over a period in a reference frame moving with filament midpoint, the numbers are related to Equation (11).

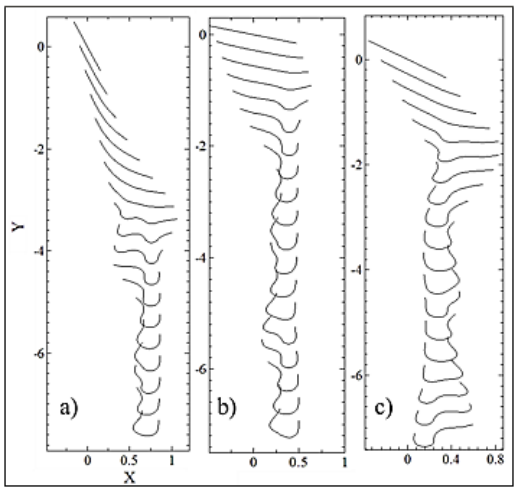

Figure 8. The motion of HF-filament in a) $\theta_0 = \theta.4\pi$, b) $\theta_0 = \theta.1\pi$, c) $\theta_0 = \theta.25\pi$, each sub-figure shows nineteen time-steps.

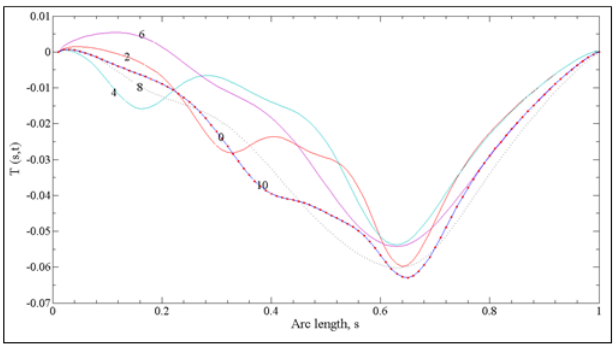

Figure 9. Variation of internal tension for HF-filament over a period, the numbers is related to Equation (11).

4. Conclusion

In this paper, the dynamics of slim flexible particles, which are refereed as filaments, have been studied. Two types of filament regimenting in quiescent fluid flow are encountered to our investigation. As well as Li et al.[21] suggestions we utilized two dimensionless parameters, elasto-gravitation number and Slenderness-parameter, to characterize the problems. In order to model the interaction between fluid and solid the non-local approach employed. Besides, we used semi-implicit approach suggested by Tornberg and Shelley [11] to treat the stiffness of non-local operator integral equation.

The behaviors of moderately and highly flexible filament are studied under different initial angles and the following results are obtained from the results:

- During the sedimentation of a moderately flexible filament, the filament tends to meet an equilibrium situation, at this point the trajectory of mid-point leans to a vertical line, the lateral velocity goes to zero, the filament deforms to a constant U-shape form, and the downward filament velocity gives a constant value.
- During the sedimentation of highly flexible filament, the filament shows an elastic bucking instability, the trajectory of mid-point tends to an oblique asymptote. Because of non-symmetrical deformation happening along the filament, the filament has a permanent periodic motion which leads to a perpetual lateral drift.

There are two points should be noted here; firstly, the effects related to re-approach of filament are not included in our model. These effects would be significant when two parts of filament get close to each other. Secondly, as we know the Euler-Bernoulli equation is a linear zed approach, so that, it will lose its accuracy when large curvature is imposed to the filament. We used this theory without any consideration to these limitations. In our future research we will work on filament sedimentation using non-linear models.

5. Acknowledgement

This research was supported by National Elites Foundation and MUT.

6. References

1. Tian FB, Dai H, Luo H, Doyle JF, Rousseau B. Fluid–structure interaction involving large deformations: 3D simu-

lations and applications to biological systems. J Comput Phys. 2014; 258(3):451–69.
2. Dai H, Luo H, Doyle JF. Dynamic pitching of an elastic rectangular wing in hovering motion. J Fluid Mech. 2012; 693(1):473–99.
3. Stockie JM, Green SI. Simulating the motion of flexible pulp fibers using the immersed boundary method. J Comput Phys. 1998; 147(1):147–65.
4. Stokes GG. On the effect of the internal friction of fluids on the motion of pendulums. Transactions of the Cambridge Philosophical Society. 1851; 9:8–106.
5. Stimson M, Jeffery GB. The motion of two spheres in viscous fluid. Proceedings of the royal society of London. Ser A. 1996; 111:110–6.
6. Jeffery GB. On the motion of ellipsoidal particles immersed in a viscous fluid. Proceedings of the royal society of London. Ser A. 1922; 102:161–99.
7. Jung S, Spagnolie SE, Parikh K, Shelley M, Tornberg AK. Periodic sedimentation in a Stokesian fluid. Phys Rev E. 2006; 74(3):353–72.
8. Cox RG. The motion of long slender bodies in a viscos fluid: Part 1. General theory. J Fluid Mech. 1970; 44(4):791–810.
9. Lighthill J. Flagellar hydrodynamics. The John von Neumann Lecture. SIAM Review. 1976; 18(2):161–230.
10. Johnson RE. An improved slender-body theory for Stokes flow. J Fluid Mech. 1980; 99(1):411–31.
11. Tornberg AK, Shelley MJ. Simulating the dynamics and interactions of flexible fibers in Stokes flows. J Comput Phys. 2004; 196(1):8–40.
12. Monfared V, Fazaeli D, Daneshmand S, Shafaghatian N. Simulation of elasto-plastic deformations in composites by flow rules. Indian Journal of Science and Technology. 2014; 7(2):180–4.
13. Gao T, Tseng YH, Lu XY. An improved hybrid Cartesian/immersed boundary method for fluid-solid flows. Int J Numer Meth Fluid. 2007; 55(12):1189–211.
14. Peskin CS. Numerical analysis of blood flow in the heart. J Comput Phys. 1977; 25(1):220–52.
15. Zhu L, Peskin CS. Simulation of a flapping flexible filament in a flowing soap film by the immersed boundary method. J Comput Phys. 2002; 179(2):452–68.
16. Delmotte B, Climent E, Plouraboue F. A general formulation of bead models applied to flexible fibers and active filaments at low Reynolds number. J Comput Phys. 2015; 286(1):14–37.
17. Becker L, Shelley MJ. The instability of elastic filaments in shear flow yields first normal stress differences. Phys Rev Lett. 2001; 87:198–210.
18. Dehghani H, Shojaei B. Simulating the sedimentation of single flexible filament in Stokes flow. Int J Sci Basic Appl Res. 2014; 3(SP):303–11.
19. Keller JB, Rubinow SI. Slender-body theory for slow viscous flow. J Fluid Mech. 1976; 75(4):705–14.
20. Shelley MJ, Ueda T. The Stokesian hydrodynamics of flexing stretching filaments. Physica D: Nonlinear phenomena. 2000; 146(1):221–45.
21. Li L, Manikantan H, Saintillan D, Spagnolie SE. The sedimentation of flexible filaments. J Fluid Mech. 2013; 735(2):705–36.
22. Batchelor GK. Slender-body theory for particles of arbitrary cross-section in Stokes flow. J Fluid Mech. 1970; 44(3):419–40.
23. Tian FB, Dai H, Luo H, Doyle JF, Rousseau B. Fluid–structure interaction involving large deformations: 3D simulations and applications to biological systems. J Comput Phys. 2014; 258(3):451–69.
24. Dai H, Luo H, Doyle JF. Dynamic pitching of an elastic rectangular wing in hovering motion. J Fluid Mech. 2012; 693(1):473–99.